

Electronic Supplementary Information

Triboelectric Generator made of Mechanically Robust PVDF Film as Self-powered Autonomous Sensor for Wireless Transmission Based Remote Security System

Bushara Fatma^{*a}, Shashikant Gupta^a, Chandrachur Chatterjee^a, Ritamay Bhunia^{a,b},
Vivek Verma^a, Ashish Garg^a

^a Department of Material Science and Engineering, Indian Institute of Technology Kanpur, Kanpur 208016, India.

^b Department of Materials Engineering, Indian Institute of Science, Bengaluru 560012, Karnataka, India.

* Corresponding author

E-mail address: bushara@iitk.ac.in; busharafatma@gmail.com (B. Fatma)

Table S1. Comparison between our device output performance and other devices reported in the literature.

S. No	Negative Triboelectric Material	Positive Triboelectric Material	Preparation method	Electrode	Mode of Operation	Output Voltage (V)	Output Current (μ A)	Current Density (μ A/cm ²)	Power Density (mW/m ²)	Application	Ref.
1	Silicone Rubber film	PVDF- HFP+ BCZT	Commercial, Electro-spinning	Ag/Ni Tape	Contact-separation	~ 42	~ 0.75	0.17	161.7	Wearable biomechanical sensor	1
2	PVDF+Fe ₃ O ₄	Al	Electro-spinning	Al	Contact-separation	~138	~ 6	0.23	---	---	2
3	PVDF+PDMS+ ZnO	Al	Solution casting	C, Al	Contact-separation	~35.7	0.28	---	70	---	3
4	PTFE	ZnO+PVDF	Solution Casting	Au	Contact-separation	~75	---	~0.4	245	---	4
5	PVDF	Mustard seed	Electro-spinning	Al, ITO	Contact-separation	~ 81	---	~2	334	---	5
6	Polyimide	PVDF-TrFE coated paper	Spin coating	Cu tape, pencil trace	Contact-separation (grating structure)	~ 100	~ 11	---	64	---	6
7	PVDF-TrFE	Conductive fabric	Electro-spinning	Al foil, conductive fabric	Contact-separation	~ 160	~ 17	---	1600	---	7
8	PVDF+Ag NP	Nylon	Electro-spinning	Al foil	Contact-separation	~ 240	~ 12	---	---	---	8
9	PVDF-TrFE, Kapton, Cu, PDMS, PET (Hybrid Nanogenerator)		Electrospinning, commercial, sputter-coated, spin-coated, commercial	Cu, ITO	Contact-separation	~361	~ 11	---	0.441 mW	---	9
10	PVDF+ Maghemite	PET	Spin coating, commercial	ITO	Contact-separation	~250	~5	0.35	117	Harvesting high frequency vibrations and biomechanical motion	10
11	FEP	Al Foil	Commercial	Silver paste, Al foil	Contact-separation	~ 360	---	~0.75	833	Wind energy Harvesting	11
12	PVDF	Bacterial cellulose	Solution casting	Al Tape	Contact-separation	~410	~14.8	0.57	1360	Self-powered autonomous wireless motion sensor	This Work

Table S2. Saturated salt solutions and their corresponding humidity. *10% relative humidity is obtained using silica gel (without using the saturated salt solution)

S. No	Saturated Salt Solution	Relative Humidity (%)
1.	MgCl ₂	33±1
2.	MgNO ₃	54±1
3.	NaCl	70±2
4.	KCl	81±2
5.	KNO ₃	95±2
7.	Silica gel*	10±1

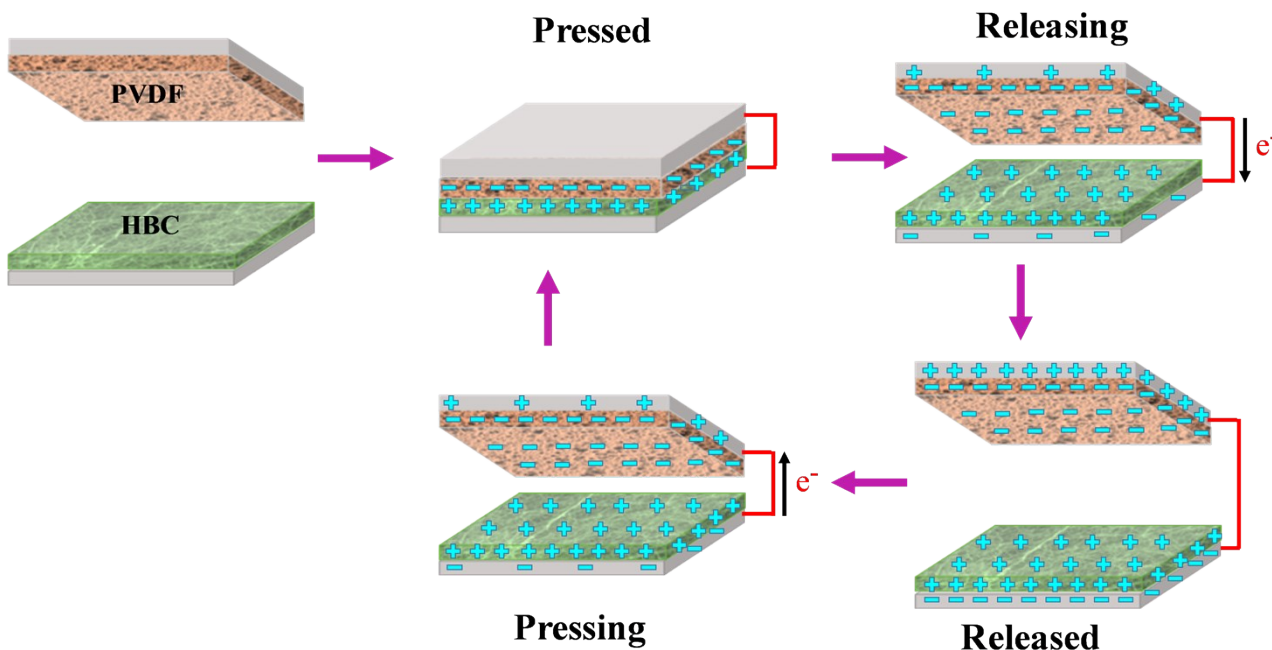


Fig. S1 Schematic of the power generation mechanism of TENG based on top PVDF and bottom BC films as negative and positive triboelectric layers.

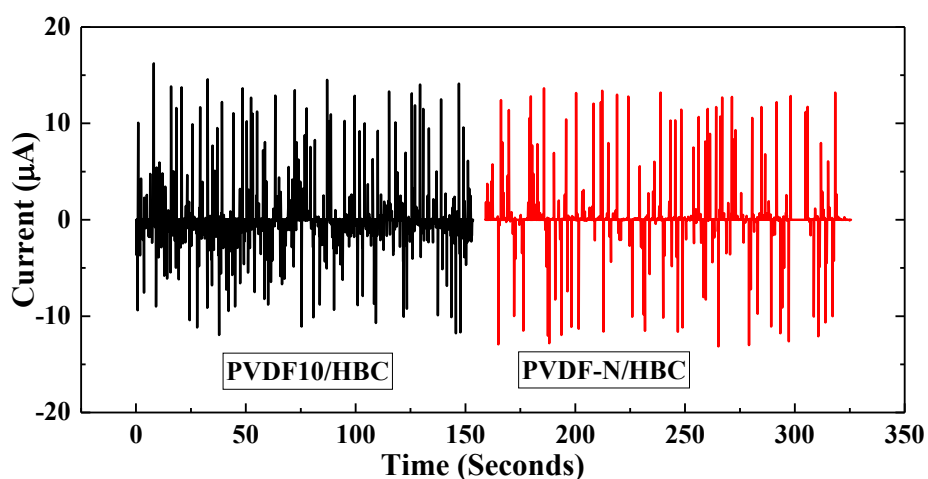


Fig. S2 Current output of device containing PVDF film prepared at 10% relative humidity using silica gel and PVDF film prepared in a glove box with BC as a positive triboelectric layer.

Table S3. Characteristic FTIR absorption bands of α -, β - and γ -phase.¹²⁻¹⁶ Peaks observed in our study are written in bold letters.

α -phase (cm ⁻¹)	β - phase (cm ⁻¹)	γ -phase (cm ⁻¹)
408	445	431
489,490	467	440
532	510	512
614,615	745	776
763,764	840	812
766	884	833
795,796	1175	838,840
855	1275	883
975,976	1279	950
1149		1117
1210		1233

Increasing the spacer distance from 2 mm to 8 mm enhances the output voltage from ~175 V to ~410 V at 5.2 Hz contact frequency (Fig. S3). The enhancement in the device performance with increasing the spacer distance can be attributed to the faster relative velocity during contact and separation between PVDF10 and BC films, leading to a faster charge transfer.

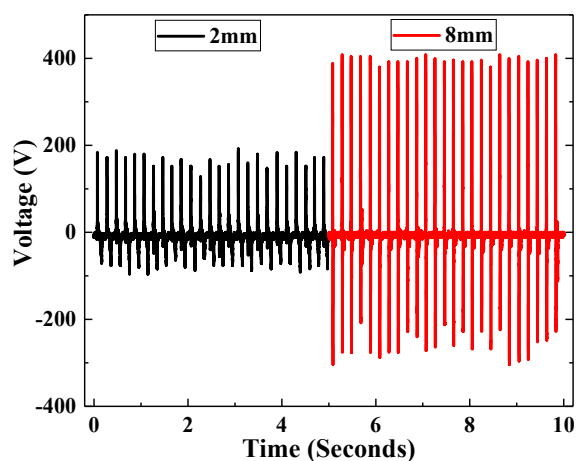


Fig. S3 Open-circuit voltage output of PVDF10 based TEG device at different spacer thickness of 2 mm and 8 mm.

All the TEGs were used to charge 1 μF capacitor with rectified output voltage of all the devices plotted in Fig. S4a. It takes only 40 sec for PVDF10 based TEG to completely charge 1 μF capacitor close to 100 V while PVDF33 based TEG takes 60 sec i.e. one minute to charge the capacitor completely. In contrast, PVDF54 based TEG takes 200 sec i.e. more than 3 minutes to charge the capacitor to a value of 80 V and then saturates. This confirms the fastest charging ability of PVDF10 based TEG. Later the best performing TEG based on PVDF10 was used to charge capacitors of different capacitance (Fig. S4b). The obtained charging voltage for each is shown in Fig. S4b. Within 2 minutes, the TEG was able to store 39 V, 13.3 V, 7.5 V, 3.2 V for 10 μF , 22 μF , 47 μF , and 100 μF capacitors, respectively. The output of PVDF10/BC TEG is high enough to be directly used as a power source for various applications. To evaluate the practical application of TEGs, we also lit up a group of LEDs connected in series, without the use of capacitor by harvesting biomechanical motion induced contact and separation. Fig. S4c shows the actual image of LEDs being in ON condition in response to the foot strike. Moreover, the device response is obtained even at low frequency (Video S1). Thus, it can be concluded that these PVDF/BC based TEGs show great prospects in scavenging energy from biomechanical motion such as foot strike to generate electricity for pedestrians in case of emergency.

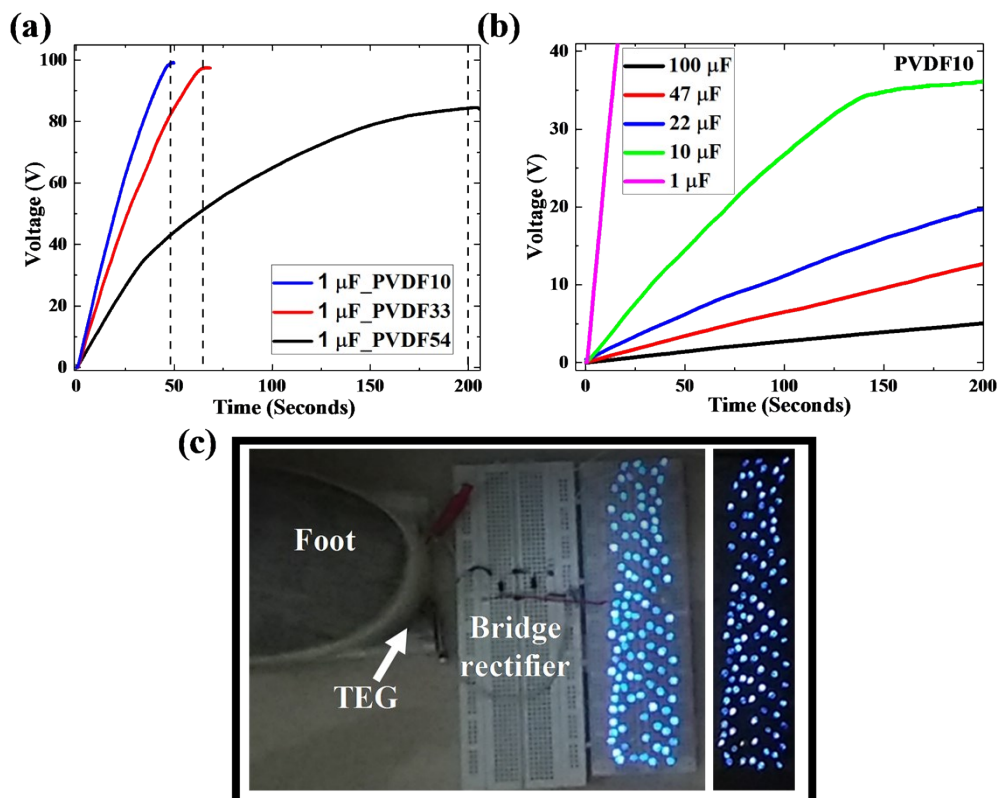


Fig. S4 (a) Capacitor charging plot of 1 μ F capacitor for PVDF10, PVDF33 and PVDF54 based TEG devices and (b) charging capability of PVDF10 based device to charge different capacitors. (c) Harvesting of biomechanical motion using low frequency foot strike to light up 100+ LEDs.

This device output is sufficient to light up SMD (surface mounted devices) LEDs. These are surface mounted LEDs that are used in computers and smartphones as indicators. SMD is mostly used in tiny devices where availability of free space is a constraint. Fig. S5a shows lighting up of SMD LEDs in response to the manual tapping driven contact and separation of layers. Other than lighting up of LEDs, the practical application of best performing TEG includes lighting up of 5-bit 7 segment LCD display. Fig. S5b shows the ON and OFF condition of LCD in response to the contact and separation of triboelectric layers. Video S2 shows continuous lighting up of LCD without a capacitor.

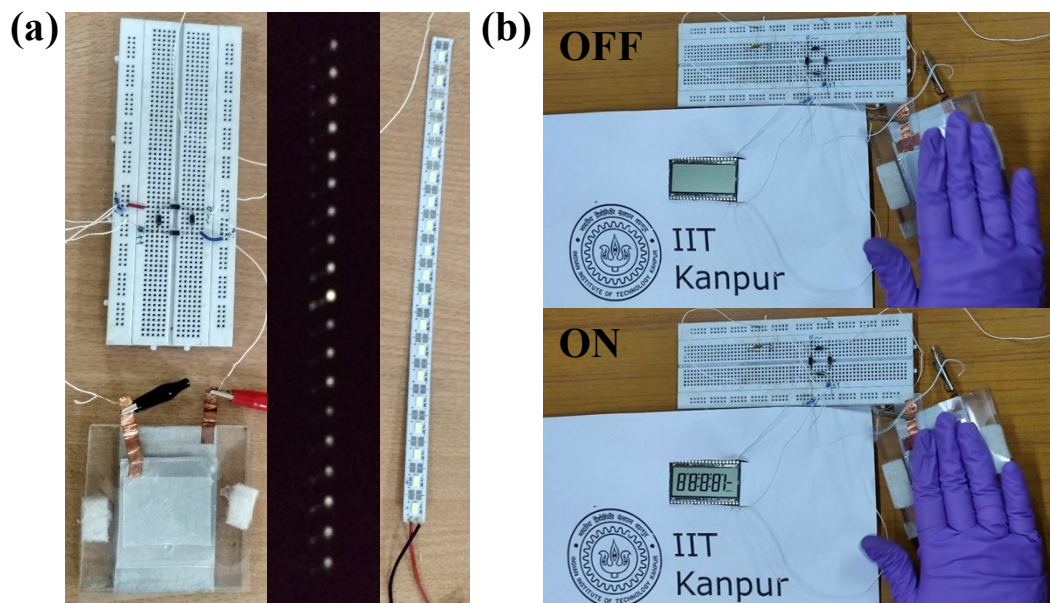


Fig. S5 Lighting up of (a) SMD LEDs and (b) 5-bit 7 segment LCD display by tapping PVDF10/BC device.

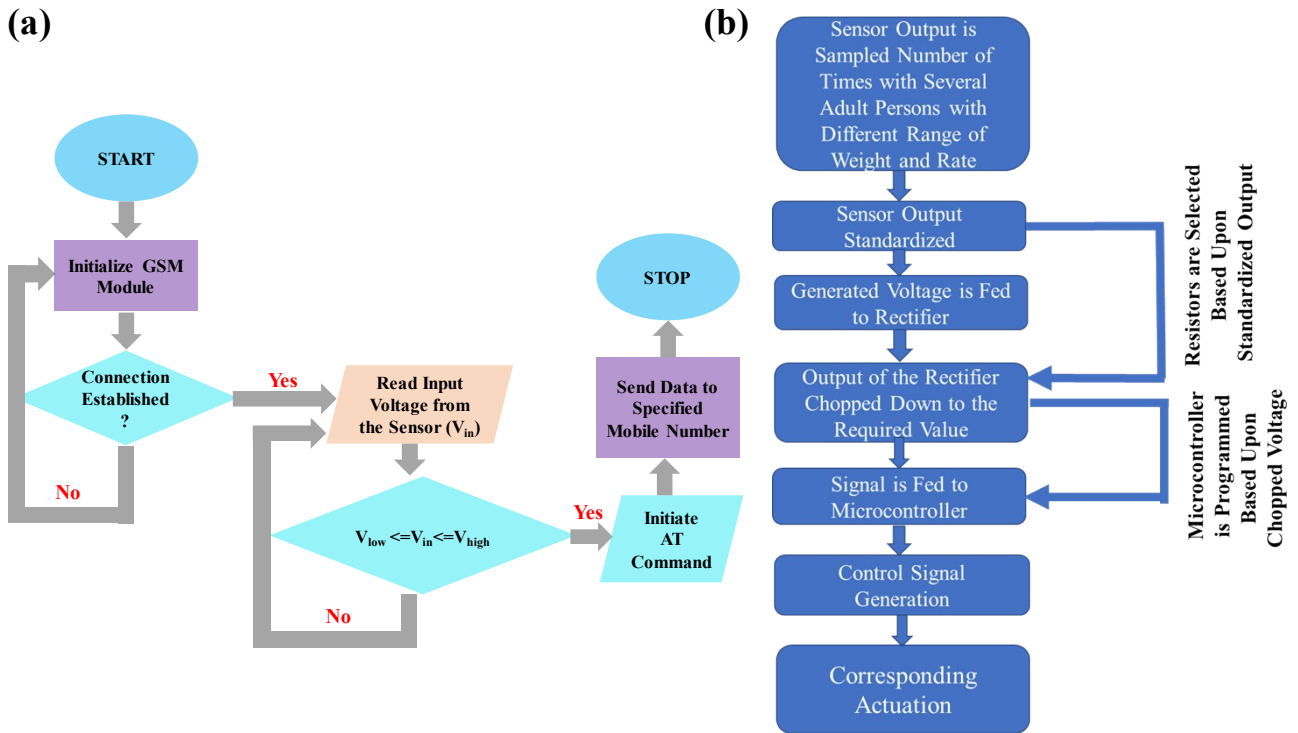


Fig. S6 (a) Flow chart of the embedded code developed for the detection system showing the detailed working mechanism of a remote intruder alarm system. (b) Flow chart for the working mechanism of remote anti-theft alarm system using PVDF10/BC TEG as a self-powered motion detector.

List of Videos

Video S1. More than hundred LEDs were directly lit up in response to the foot strike using TEG.

Video S2. 5-bit 7 segment LCD display was lit up using TEG without a capacitor.

Video S3. Using TEG as self-powered motion sensor for wireless transmission based remote security system.

References

1. Y. Wu, J. Qu, W. A. Daoud, L. Wang and T. Qi, *J. Mater. Chem. B*, 2019, **7**, 13347-13355.
2. J.-S. Im and I.-K. Park, *ACS Appl. Mater. Interfaces*, 2018, **10**, 25660-25665.
3. X. Yang and W. A. Daoud, *Adv. Funct. Mater.*, 2016, **26**, 8194-8201.
4. H. H. Singh and N. Khare, *Nano Energy*, 2018, **51**, 216-222.
5. S. K. Singh, P. Kumar, R. Magdum, U. Khandelwal, S. Deswal, Y. More, S. Muduli, R. Boomishankar, S. Pandit and S. Ogale, *ACS Appl. Bio Mater.*, 2019.
6. S. Jang, H. Kim and J. H. Oh, *Nanoscale*, 2017, **9**, 13034-13041.
7. S. Jang, H. Kim, Y. Kim, B. J. Kang and J. H. Oh, *Appl. Phys. Lett.*, 2016, **108**, 143901.
8. S. Cheon, H. Kang, H. Kim, Y. Son, J. Y. Lee, H.-J. Shin, S.-W. Kim and J. H. Cho, *Adv. Funct. Mater.*, 2018, **28**, 1703778.
9. X. Chen, M. Han, H. Chen, X. Cheng, Y. Song, Z. Su, Y. Jiang and H. Zhang, *Nanoscale*, 2017, **9**, 1263-1270.
10. B. Fatma, R. Bhunia, S. Gupta, A. Verma, V. Verma and A. Garg, *ACS Sustainable Chem. Eng.*, 2019.
11. H. Zhang, S. Feng, D. He, Y. Xu, M. Yang and J. Bai, *Nano Energy*, 2018, **48**, 256-265.
12. S. Lanceros-Méndez, J. F. Mano, A. M. Costa and V. H. Schmidt, *Journal of Macromolecular Science, Part B*, 2001, **40**, 517-527.
13. A. C. Lopes, C. M. Costa, C. J. Tavares, I. C. Neves and S. Lanceros-Mendez, *The Journal of Physical Chemistry C*, 2011, **115**, 18076-18082.
14. P. Martins, A. Lopes and S. Lanceros-Méndez, *Progress in Polymer Science*, 2014, **39**, 683-706.
15. M. Benz, W. B. Euler and O. J. Gregory, *Langmuir*, 2001, **17**, 239-243.
16. A. Salimi and A. Yousefi, *Journal of Polymer Science Part B: Polymer Physics*, 2004, **42**, 3487-3495.